

Desmoglein-2 is overexpressed in non-small cell lung cancer tissues and its knockdown suppresses NSCLC growth by regulation of p27 and CDK2

Feng Cai¹ · Qingqing Zhu¹ · Yingying Miao¹ · Simei Shen¹ · Xin Su¹ · Yi Shi¹

Received: 27 August 2016 / Accepted: 31 August 2016 / Published online: 14 September 2016
© Springer-Verlag Berlin Heidelberg 2016

Abstract

Purpose Desmoglein-2 (Dsg2) is a cell adhesion protein of the cadherin superfamily. Altered Dsg2 expression is associated with tumorigenesis. This study determined Dsg2 expression in non-small cell lung cancer (NSCLC) tissue specimens for association with clinicopathological and survival data and then assessed the effect of Dsg2 knockdown on regulation of NSCLC cell malignant behaviors in vitro and in nude mouse xenografts.

Methods qRT-PCR and Western blot were used to detect Dsg2 expression in 28 paired NSCLC and normal tissue samples. Immunohistochemistry was used to detect Dsg2 expression in 70 cases of paraffin-embedded NSCLC tissues. NSCLC A549, H1703, and H1299 cells were cultured with Dsg2 knockdown performed using Dsg2 siRNA. Cell viability, cell cycle, apoptosis, and colony formation were assessed. siRNA-transfected A549 cells were also used to generate tumor xenografts in nude mice.

Results Both Dsg2 mRNA and protein were highly expressed in NSCLC tissues and associated with NSCLC size, but not with overall survival of patients. Moreover, knockdown of Dsg2 expression reduced NSCLC cell proliferation and arrested them at the G1 phase of the cell

cycle, but did not significantly affect NSCLC cell apoptosis. Dsg2 knockdown downregulated cyclin-dependent kinase 2 expression and upregulated p27 expression. Nude mouse xenograft assays showed that Dsg2 knockdown inhibited NSCLC xenograft growth in vivo.

Conclusion This study revealed the importance of Dsg2 in suppression of NSCLC development and progression. Further studies will explore whether restoration of Dsg2 expression is a novel strategy in control of NSCLC.

Keywords NSCLC · Desmoglein-2 · Tumor cell proliferation · Cell cycle regulation

Abbreviations

AC	Adenocarcinomas
BCC	Basal cell carcinomas
Dsg	Desmoglein
NSCLC	Non-small cell lung cancer
qRT-PCR	Quantitative reverse-transcription polymerase chain reaction
SCC	Squamous cell carcinomas
siRNA	Small interfering RNAs
TNM	Tumor–nodes–metastasis

Electronic supplementary material The online version of this article (doi:10.1007/s00432-016-2250-0) contains supplementary material, which is available to authorized users.

✉ Xin Su
suxinjs@163.com

✉ Yi Shi
shiyi56@126.com

¹ Department of Respiratory Medicine, Jinling Hospital, Medical School of Nanjing University, 305 East Zhongshan Road, Nanjing 210002, Jiangsu, China

Introduction

Lung cancer is still the leading cause of cancer-related deaths in men and becomes the leading cause of cancer-related deaths in women in the world. In 2008, lung cancer accounted for an estimated 1.6 million new cancer cases and 1.4 million cancer-related deaths globally (Jemal et al. 2011). By 2012, new lung cancer cases were estimated to have increased to 1.8 million globally (Torre et al. 2015). Fortunately, in Western countries with effective tobacco

control and prevention, lung cancer mortality has shown a trend to decrease in men and has reached a plateau in women (Siegel et al. 2016; Torre et al. 2015). However, in developing countries like China, lung cancer mortality and morbidity are continuously increasing due to tobacco epidemic and air pollution (Chen et al. 2016; Torre et al. 2015). Histologically, non-small cell lung cancer (NSCLC) represents up to 85 % of all lung cancer cases and NSCLC is usually diagnosed at advanced stages of the disease, at which time curable surgery is not a treatment option. Thus, research into the molecular mechanisms underlying lung tumorigenesis and cancer progression could lead to improvements in early diagnosis, prognosis, and treatment of NSCLC clinically.

Desmoglein-2 (Dsg2) is a cell adhesion protein of the cadherin superfamily and is crucial for cardiomyocyte cohesion and functions (Schlipp et al. 2014). The cadherin superfamily of proteins is a class of type 1 transmembrane proteins that contains cadherins, protocadherins, desmogleins, and desmocollins. The purpose of these proteins is to regulate cell–cell contact to adjacent cells (Angst et al. 2001; Hulpiau and van Roy 2009). The subfamily of desmosomal cadherins is an important component of desmosomes and consists of desmogleins (Dsg) and desmocollins (Broussard et al. 2015). Altered expression or function of desmosomal cadherins is associated with human tumorigenesis, such as skin cancer, esophageal squamous cell carcinoma (SCC), colon cancer, and lung cancer (Brown and Wan 2015; Fang et al. 2014; Fukuoka et al. 2007; Jiang et al. 2011; Johnson et al. 2014; Kamekura et al. 2014; Kolegraff et al. 2011). Dsg2 is the only desmoglein isoform expressed in cardiomyocytes, and Dsg2 gene mutations have been associated with arrhythmogenic right ventricular cardiomyopathy (Kamekura et al. 2014; Pilichou et al. 2006) and with pemphigus lesions (Iwatsuki et al. 1999; Syrris et al. 2007). However, to date, the role of Dsg2 in human cancer is uncertain. For example, Dsg2 expression was downregulated in diffuse-type gastric cancer, prostate cancer, and pancreatic cancer (Barber et al. 2014; Ramani et al. 2008; Yashiro et al. 2006). Davie et al. (1997) showed Dsg2 to be a putative tumor suppressor and to reduce cell aggregation, invasion, and motility in human breast cancer cells. In contrast, other studies reported that Dsg2 was overexpressed in skin SCC and basal cell carcinoma (BCC) (Brennan and Mahoney 2009), while loss of Dsg2 suppressed colon cancer cell proliferation, suggesting an oncogenic function of Dsg2 protein (Kamekura et al. 2014). In NSCLC, previous GeneChip cDNA array data showed that Dsg2 was overexpressed in NSCLC tissues compared with adjacent normal lung tissues (Fukuoka et al. 2007).

In this study, we detected Dsg2 expression in NSCLC tissue specimens using qRT-PCR, Western blot, and immunohistochemistry and associated Dsg2 expression

with clinicopathological and survival data from NSCLC patients. We then assessed the effects of Dsg2 knockdown using Dsg2 siRNA on the regulation of NSCLC cell malignant behaviors in vitro and in nude mouse xenografts.

Materials and methods

Patients and tissue samples

This study was approved by the Institutional Review Board of Jinling Hospital, Nanjing University School of Medicine (Nanjing, China), and all patients provided a written informed consent form before being enrolled into this study. We prospectively collected paired NSCLC and adjacent normal tissues from 28 patients who underwent surgical NSCLC resection in the Department of Thoracic Surgery between September 2014 and November 2014. We also retrospectively collected NSCLC tissues samples from 70 NSCLC patients who received primary care in our hospital between June 2007 and November 2008. The last follow-up of these patients was in February 2015, and the median follow-up duration was 84.5 months (ranged between 75 and 94 months). For this study, paraffin-embedded tissue blocks were retrieved from Department of Pathology and sectioned for immunohistochemistry.

Immunohistochemistry

Formalin-fixed and paraffin-embedded tissue sections were deparaffinized in xylene for 10 min each and rehydrated in a series of ethanol solution (100–50 %). The tissue sections were then subjected to antigen retrieval with 0.01 M citric buffer in a microwave for 10 min, followed by blocking of tissue endogenous peroxidase activity with H₂O₂ treatment for 30 min at room temperature. Non-specific binding sites were blocked by incubation of tissue sections in 10 % goat serum for 30 min. Tissue sections were then incubated with a primary antibody against human Dsg2 (Abcam, Cambridge, MA, USA) at a dilution of 1:200, or Ki67 (Abcam) at a dilution of 1:100 at 4 °C overnight. On the next day, tissue sections were washed three times with phosphate-buffered saline (PBS) and then incubated with a secondary antibody (Boster, Beijing, China) at room temperature for 30 min. After further washes with PBS, tissue sections were incubated with the avidin–biotin complex solution (Boster, Beijing, China) in the dark for 30 min. The color reaction was performed using 3,3'-diaminobenzidine (DAB) solution, and the tissue sections counterstained with hematoxylin and mounted with a coverslip.

Immunostained tissue sections were then reviewed and scored independently by two pathologists without knowledge of the patient characteristics. Any discrepancies were

resolved by consensus review. The percentage of staining and the staining intensity were recorded as follows: 0, $\leq 5\%$; 1 = 6–20%; 2 = 21–50%; and 3 $\geq 50\%$ of tumor cells stained positive, while staining intensity was scored as: 0 = no staining; 1 = weak staining; 2 = moderate staining; and 3 = strong staining. These two scores were then added together to form a final staining score categorized as low (<3) or high (≥ 3) expression of Dsg2.

Cell lines and culture

NSCLC cell lines A549, H1703, and H1299 were obtained from the Institute of Biochemistry and Cell Biology of the Chinese Academy of Sciences (Shanghai, China) and cultured in RPMI1640 culture medium (Invitrogen, Carlsbad, CA, USA) supplemented with 10% heat-inactivated fetal bovine serum (FBS, Invitrogen), 100 U/ml penicillin, and 100 mg/ml streptomycin (KeyGEN BioTECH, Nanjing, China) in a humidified incubator with 5% CO₂ at 37 °C.

RNA isolation and qRT-PCR

Total RNA was isolated from frozen tissues or cultured cells using TRIzol reagent (Invitrogen) and reversely transcribed into complementary DNA using a cDNA synthesis kit (Takara Bio, Dalian, China) according to the manufacturers' protocols. qPCR amplification was conducted using the ABI QuantStudio[®]3 real-time PCR system (Applied Biosystems, Foster City, CA, USA) with SYBR reagent (Takara Bio). The primer sequences were: human β -actin, 5'-AGCGAGCATCCCCAAAGTT-3' and 5'-GGGCACGAAGGCTCATCATT-3' according to a previous study (Fang et al. 2013), and human Dsg2, 5'-ATGACGGCTAGGAACACCAC-3' and 5'-GGGTCAGTTTGTGGCTGACT-3' (Vite et al. 2013). The qPCR conditions were set to 95 °C for 30 s followed by 40 cycles of 95 °C for 30 s and 60 °C for 31 s. Levels of Dsg2 mRNA were quantified using $2^{(-\Delta Ct)}$ and normalized against β -actin.

Protein extraction and Western blot

Tissue or cell samples were lysed in a radioimmunoprecipitation assay buffer (Beyotime, Haimen, Jiangsu, China) containing protease inhibitor cocktail (Roche, Basel, Switzerland). After quantitation with the bicinchoninic acid (BCA) protein assay method, equal amounts of protein samples were separated in 8 or 12% sodium dodecyl sulfate–polyacrylamide gel electrophoresis (SDS-PAGE) gels and then blotted onto PVDF Immobilon-P membranes (Millipore, Bedford, MA, USA). The membranes were then blocked in 5% nonfat milk in Tris-based saline-Tween 20 (TBS-T) for 1 h at room temperature and further incubated with the primary antibody overnight at 4 °C. The primary

antibodies were anti-Dsg2 (1:5000; Abcam), anti- β -tubulin (1:1000; Cell Signaling Technology, Danvers, MA, USA), anti-p27 (1:1000; Cell Signaling Technology), and anti-cyclin-dependent kinase 2 (CDK2, 1:1000; Cell Signaling Technology). On the next day, the membranes were washed with TBS-T three times and incubated with a horseradish peroxidase-conjugated secondary antibody (Cell Signaling Technology) for 2 h at room temperature. Protein bands were visualized by using a chemiluminescence kit (Millipore) and quantified using the Tanon Automatic Chemiluminescence Western Blot Imaging system (Tanon, Shanghai, China).

siRNA and transfection of cells

The sequences of Dsg2 siRNA were 5'-CCUCCAGU GUUCUACCUAATT-3' (sense) and 5'-UUAGGUAGA ACACUGGAGGTT-3' (antisense), while those of negative control siRNA were 5'-UUCUCCGAACGUGUCAC GUTT-3' (sense) and 5'-ACGUGACACGUUCGGAGA ATT-3' (antisense). These double-stranded siRNAs were synthesized by GenePharma (Shanghai, China) and transfected into cells for 48 h using Lipofectamine 2000 Transfection Reagent (Invitrogen). After that, cells were analyzed for knockdown of Dsg2 expression using qPCR and Western blot.

CCK-8 cell growth assay

Dsg2 and negative control siRNA-transfected cells were seeded into a 96-well plate at a density of 3000 cells per well and incubated in a humidified incubator at 37 °C with 5% CO₂ for up to 5 days. At the end of each experiment, 20 μ l of CCK-8 solution was added to the cell culture and the cells were further incubated at 37 °C for 2 h. The absorbance rate was then measured at 450 nm using an epoch microplate spectrophotometer (BioTek Instruments Inc., Vermont, USA). The data were expressed as mean \pm SD and summarized as percentage of control.

5-ethynyl-2'-deoxyuridine (EdU) incorporation assay

Dsg2 and negative control siRNA-transfected cells were seeded into a 96-well plate at a density of 3000 cells per well and incubated in a humidified incubator at 37 °C with 5% CO₂ for 24 h. The cells were then exposed to 50 mM of EdU (RiboBio, Guangdong, China) for 2 h at 37 °C. Next, the cells were washed with ice-cold PBS and fixed in 4% formaldehyde for 15 min before permeabilization with 0.5% Triton X-100 in PBS. Cells were reacted with 1 \times Apollo[®] reaction cocktail for 30 min at room temperature and subsequently stained with Hoechst33342 (RiboBio) for 30 min before visualization under a fluorescent microscope (Carl Zeiss Jena, Oberkochen, Baden-Württemberg, Germany).

EdU incorporation rate was expressed as the ratio of EdU-positive cells to total Hoechst33342-positive cells.

Flow cytometry cell cycle and apoptosis assays

Dsg2 and negative control siRNA-transfected cells were seeded into a 6-well plate at a density of $1.5\text{--}2.5 \times 10^5$ cells per well and incubated in a humidified incubator at 37 °C with 5 % CO₂ for 3 days. The cells were then fixed in 70 % ethanol and stained using the CycleTEST™ PLUS DNA reagent kit (BD Biosciences, San Jose, CA, USA) for 30 min at 4 °C according to the manufacturer's protocol. Cells were detected by FACS Calibur flow cytometry (BD Biosciences) and analyzed with CellQuest software (BD Biosciences) for cell cycle distribution. For apoptosis analysis, cells were double-stained with the Annexin V FITC/PI apoptosis detection kit (BD Biosciences) according to the manufacturer's instructions and analyzed using FACS Calibur flow cytometry (BD Biosciences) and CellQuest software (BD Biosciences).

Tumor cell colony formation assay

Dsg2 and negative control siRNA-transfected cells were seeded into a 6-well plate at a density of 1500 cells per well and incubated in a humidified incubator at 37 °C with 5 % CO₂ for 2 weeks with medium change every 3 days. Cells were then fixed in 4 % formaldehyde for 15 min and then subsequently stained with 0.1 % crystal violet solution and the visible colonies counted.

Nude mouse xenograft assay

The animal protocol for this study was approved by the Institutional Animal Care and Use Committee (IACUC) of Jinling Hospital, Nanjing University School of Medicine (Nanjing, China). Four- to five-week-old male nude mice were inoculated with three millions of Dsg2 and negative control shRNA-transfected A549 cells subcutaneously in both sides of the posterior flank. The sequences of Dsg2 shRNA were 5'-CCTCCAGTGTCTACCTAA TTCAAGAGATTAGGTAGAACACTGGAGG TTTTTT-3', while those of negative control shRNA were 5'-UUCUCCGAACGUGUCACGU TTCAAGAGACGUGACACGUUCGGA GAA TTTTTT-3'. Tumor growth was monitored using calipers every 3 days, and tumor xenografts were collected 2 weeks after tumor cell injection and measured for weight and size. The tumor length (*L*) and width (*W*) were measured, and tumor volume was calculated as $1/2 LW^2$.

Statistical analysis

All statistical analyses were performed using SPSS software, version 19 (SPSS Inc., Chicago, IL, USA). The Chi-square

or Fisher's exact test was performed to analyze association of Dsg2 expression with clinicopathological features from patients, while Kaplan–Meier survival curves were used to assess association of Dsg2 expression with overall survival of patients. Moreover, comparison of two variables of the in vitro data was conducted using Student's *t* test. A *P* < 0.05 was considered to be statistically significant.

Results

Dsg2 overexpression in NSCLC tissue specimens and clinical significance

In this study, we first assessed Dsg2 expression in 28 fresh NSCLC tissue specimens using qRT-PCR and Western blot and found that the levels of Dsg2 mRNA were higher in NSCLC tissues than in normal tissues (Fig. 1a). Dsg2 overexpression in NSCLC tissues was further supported by analysis of the Oncomine® Platform data (<http://www.oncomine.org/>), in which Dsg2 mRNA levels were also higher in NSCLC than in normal lung tissues (Supplementary Fig. S1a). Western blot data on randomly selected four-paired tumor versus normal tissue specimens showed that levels of Dsg2 protein were also higher in NSCLC samples (Fig. 1b).

We then performed immunohistochemistry using an anti-human Dsg2 antibody in 70 paraffin-embedded archived tumor tissues from NSCLC patients. The patients consisted of 55 males and 15 females with a median age of 61 years (ranged between 39 and 77 years old). All patients were histologically confirmed to have NSCLC diagnosis, and no patients were treated with chemo- or radiotherapy before surgery. During follow-up, 37 patients (53 %) died of tumor-related causes, 30 (43 %) were still alive as of the last follow-up, and 3 (4 %) did not complete the follow-up. Our immunohistochemical data showed that Dsg2 protein was mainly localized on the cell membrane with some in the cytoplasm in NSCLC tissue specimens (Fig. 1c). We then associated Dsg2 expression in tumor cells with clinicopathological data from the 70 NSCLC patients (Table 1). Specifically, Dsg2 expression was associated with tumor size (Table 1, *P* = 0.044), but not statistically associated with SCC versus adenocarcinomas (76 vs. 54.3 %), or poor tumor differentiation (well/moderate vs. poor, 59.1 vs. 79.6 %). Moreover, Kaplan–Meier analysis did not show statistical association between Dsg2 expression and overall survival of NSCLC patients (Fig. 1d). However, our analysis of the Kaplan–Meier Plotter (<http://kmpplot.com/>) showed that high Dsg2 expression was associated with poor prognosis in 1926 cases of NSCLC patients [HR = 1.2 (1.05–1.36), *P* = 0.0058 using the log rank test; Supplementary Fig. 1b].

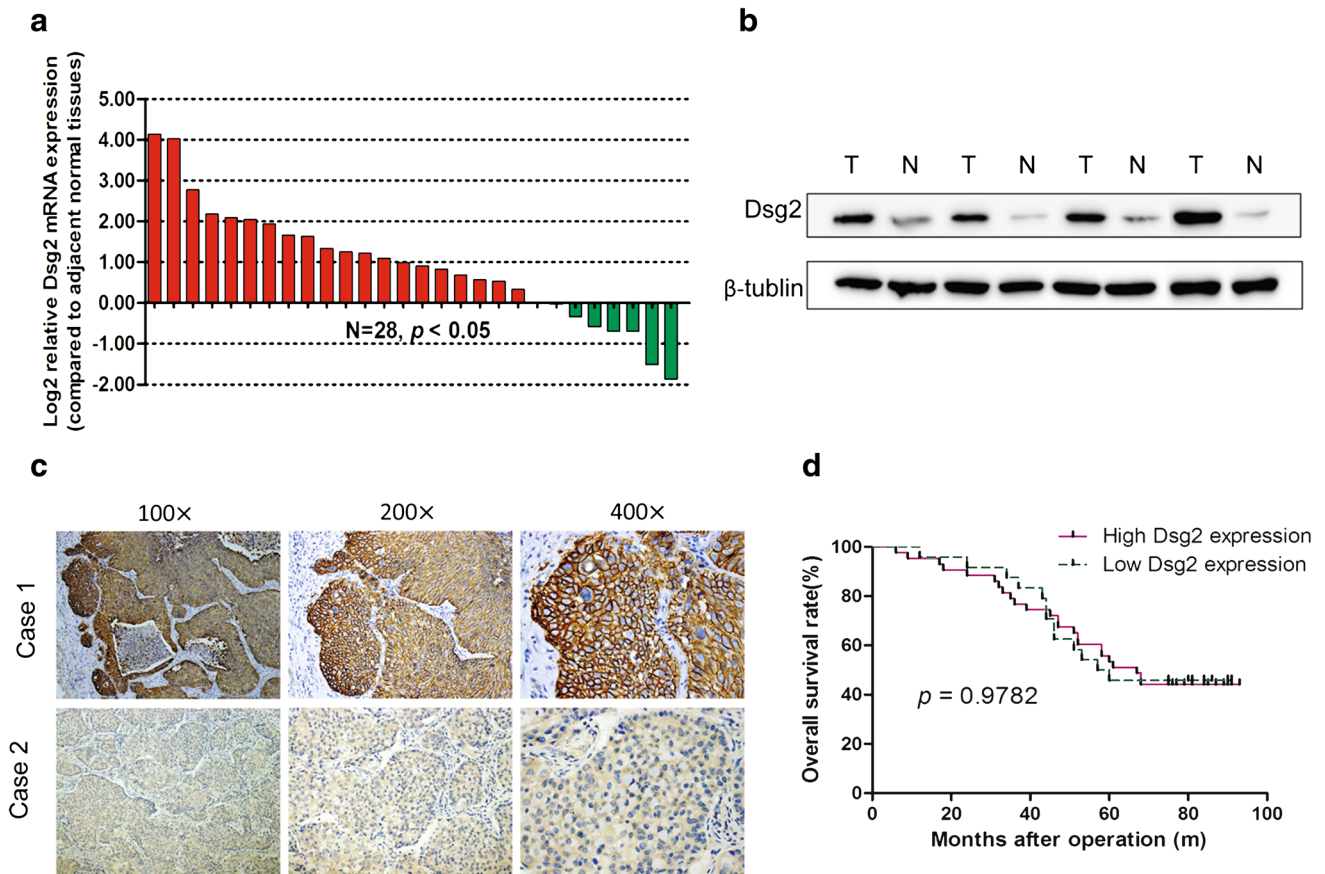


Fig. 1 Overexpression of Dsg2 mRNA and protein in NSCLC tissue specimens. **a** qRT-PCR. Fresh NSCLC and normal tissues from 28 patients were collected for qRT-PCR analysis of Dsg2 expression. **b** Western blot. Fresh NSCLC and normal tissues from 28 patients were collected for Western blot analysis of Dsg2 expression. **c** Immunohistochemistry. Paraffin blocks from 70 NSCLC patients were collected

for immunohistochemical analysis of Dsg2 expression. Representative images of Dsg2 immunostaining illustrated strong Dsg2 staining (*case 1*) or weak Dsg2 staining (*case 2*). **d** Kaplan–Meier curves of overall survival of NSCLC patients stratified by Dsg2 expression. *T* tumor, *N* normal

Effect of Dsg2 knockdown on inhibition of NSCLC cell proliferation in vitro

We evaluated the effect of Dsg2 knockdown on regulation of NSCLC cell proliferation, cell cycle distribution, and apoptosis in vitro and found that knockdown of Dsg2 in NSCLC A549, H1703, and H1299 cells (Fig. 2a, b) reduced viability of these cells (Fig. 2c). Tumor cell colony formation ability was also significantly attenuated in all three cell lines after transfection with Dsg2 siRNA compared to the negative control siRNA (Fig. 2d). EdU incorporation was also reduced in Dsg2 siRNA-transfected tumor cells (percentage of EdU-positive cells was reduced by 42.6 % in A549, 75.1 % in H1703, and 52.8 % in H1299 cells; Fig. 2e). Furthermore, cell cycle and apoptosis assays of NSCLC cell lines showed that the proportion of G1 phase cells was increased, whereas the proportion of S phase cells was decreased after knockdown of Dsg2, compared with

negative control siRNA (Fig. 3a–d). In contrast, there was no statistical difference in apoptosis between Dsg2 siRNA and negative control siRNA-transfected NSCLC cells (Fig. 3e, f).

Dsg2 regulation of CDK2 and p27 expression in NSCLC cells in vitro

We then assessed expression of proteins that regulate the G1/S checkpoint of the cell cycle. Our results showed that expression of CDK2 was significantly decreased in Dsg2 siRNA-transfected NSCLC cell lines compared with that of the negative control siRNA, whereas expression of the tumor suppressor p27 protein was increased in Dsg2 siRNA-transfected NSCLC cell lines compared with that of the negative control siRNA (Fig. 4a, b). This finding indicates that Dsg2 knockdown arrests NSCLC cell cycle progression via modulation of p27-CDK2 levels.

Table 1 Association of Dsg2 expression with clinicopathological data from 70 NSCLC patients

Variables	N	Dsg2 expression		P value ^a
		High	Low	
Age at diagnosis (years)				
<60	28	17	11	0.47
≥60	42	29	13	
Gender				
Male	55	37	18	0.59
Female	15	9	6	
Histological type				
Adenocarcinoma	25	19	16	0.12
Squamous cell carcinoma	35	19	6	
Other ^b	10	8	2	
Tumor differentiation				
Well/moderate	44	26	18	0.12
Poor	26	20	6	
Tumor size (cm)				
≤4	41	23	6	0.044
>4	29	23	14	
Lymph node metastasis				
Absent	43	29	14	0.70
Present	27	17	10	
TNM stage				
I	24	14	10	0.40
II	28	21	7	
III	18	11	7	

^a Chi-square test

^b Others included eight adenosquamous carcinoma, one large cell lung cancer, and one mucoepidermoid carcinoma

Effect of Dsg2 knockdown on suppressed NSCLC tumorigenesis in vivo

To further investigate the in vivo effect of Dsg2 knockdown on NSCLC tumorigenesis in nude mice, we performed a nude mouse xenograft assay using Dsg2 and negative control shRNA-transfected A549 cells. We found that compared to the negative control shRNA, Dsg2 knockdown significantly reduced tumor xenograft growth (Fig. 5a, b) and xenograft weight (NC vs. Dsg2 shRNA, 0.482 ± 0.033 vs. 0.182 ± 0.041 g, $P < 0.001$; Fig. 5c). Our immunohistochemical staining also confirmed Dsg2 knockdown and reduced expression of cell proliferation marker Ki-67 in Dsg2 shRNA-transfected tumor xenografts (Fig. 5d). Taken together, these assays demonstrated that Dsg2 knockdown was able to suppress NSCLC tumorigenesis in vivo, further confirming our ex vivo data.

Discussion

Our current study showed that Dsg2 is overexpressed in NSCLC tissue specimens and Dsg2 expression is associated with larger tumor size, but is not associated with overall survival of NSCLC patients. However, our analysis of the online database showed that Dsg2 expression was associated with poor prognosis in 1926 cases of NSCLC patients. Furthermore, our in vitro data revealed that Dsg2 knockdown effectively inhibited NSCLC cell proliferation and arrested tumor cells at the G1 phase of the cell cycle. At the gene level, Dsg2 knockdown downregulated CDK2 expression, but upregulated p27 expression in NSCLC cells. Our nude mouse data further confirmed our in vitro data on Dsg2 inhibition of NSCLC cell growth by showing that Dsg2 knockdown significantly reduced tumor xenograft growth weight. Our current study demonstrated that dysregulation of Dsg2 expression could lead to NSCLC development and progression, and that Dsg2 knockdown suppressed NSCLC cell malignant behaviors in vitro and in nude mice. Further studies are needed to confirm our current findings and develop a potential strategy to treat NSCLC clinically.

Desmosomal cadherins constitute the intercellular components of the desmosome–intermediate filament complex and function to adhere adjacent cells together. Since cell–cell adhesion is crucial in multiple cell process and homeostasis, desmosomes play an important role in intercellular communication and signal transduction to regulate cell proliferation, differentiation, morphogenesis, and embryonic development (Broussard et al. 2015; Garrod and Chidgey 2008). Thus, the role of desmosomes in cancer has drawn specific attention. For example, previous studies reported that certain desmosome proteins functioned as tumor suppressors by enforcement of cell–cell adhesion and prevention of epithelial to mesenchymal transition and tumor development (Dusek and Attardi 2011). However, other desmosomes, such as Dsg2, Dsg3, and Plakophilin 3 (Pkp 3), were reported to be upregulated in various human cancers (Brennan and Mahoney 2009; Breuninger et al. 2010; Fukuoka et al. 2007; Furukawa et al. 2005; Huang et al. 2010). In particular, Dsg3 was overexpressed in lung SCC and could be a useful biomarker to separate lung SCC from NSCLCs (Savci-Heijink et al. 2009). Expression of Dsg2 was upregulated in skin cancer (Brennan and Mahoney 2009), but was downregulated in gastric, prostate, and pancreatic cancers (Brennan and Mahoney 2009; Gornowicz-Porowska et al. 2011; Ramani et al. 2008; Yashiro et al. 2006). In our current study, we found overexpression of Dsg2 mRNA and protein in NSCLC tissues compared with

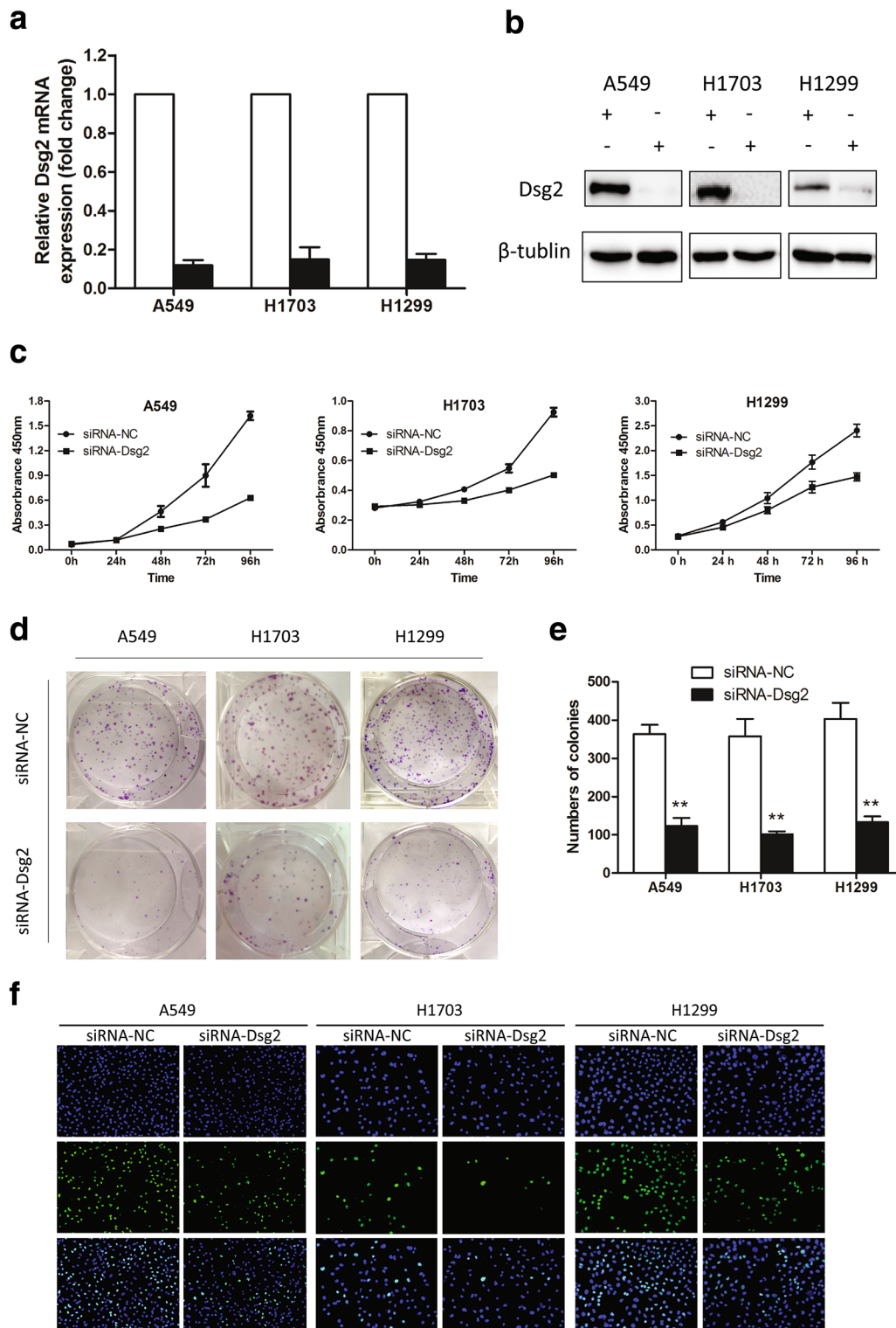


Fig. 2 Effects of Dsg2 knockdown on inhibition of NSCLC cell proliferation. **a, b** qRT-PCR and Western blot. A549, H1703, and H1299 cells were grown and transiently transfected with Dsg2 or negative control siRNA for 2 days and then subjected to qRT-PCR and Western blot analysis of Dsg2 expression. **c** Cell viability CCK-8 assay. The Dsg2-knocked down cells were grown and subjected to CCK-8 assay. **d, e** Colony formation assay. A549, H1703, and H1299 cells were grown and transiently transfected with Dsg2 or negative control

siRNA for 24 h and then subjected to a colony formation assay. **f** EdU incorporation assay. A549, H1703, and H1299 cells were grown and transiently transfected with Dsg2 or negative control siRNA for 24 h and then subjected to the EdU incorporation assay. The data represent the ratio of EdU-positive cells to total Hoechst33342-positive cells as mean ± SE of three independent experiments. **P* < 0.05 and ***P* < 0.01 using Student's *t* test

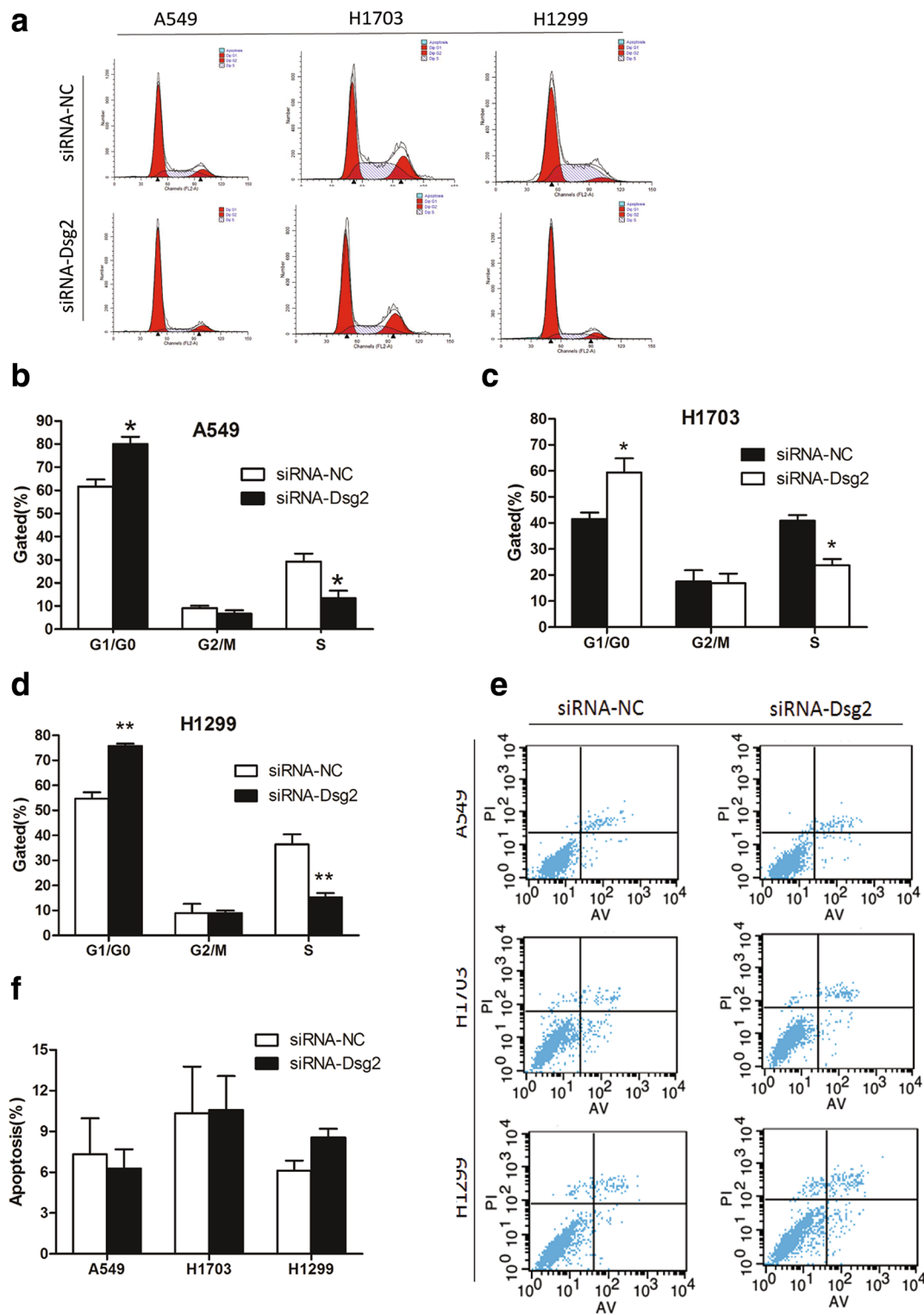


Fig. 3 Effects of Dsg2 knockdown on arrest of NSCLC cell cycle. **a** Flow cytometric cell cycle assay. A549, H1703, and H1299 cells were grown and transiently transfected with Dsg2 or negative control siRNA for 3 days and then subjected to flow cytometry cell cycle assay. **b–d** Quantified data of **a**. The data are expressed as mean \pm SE of three independent experiments. * $P < 0.05$ and ** $P < 0.01$ using

Student's *t* test. **e** Flow cytometric tumor cell apoptosis assay. A549, H1703, and H1299 cells were grown and transiently transfected with Dsg2 or negative control siRNA for 3 days and then subjected to flow cytometric tumor cell apoptosis assay. **f** Quantified data of **e**. The data are expressed as mean \pm SE of three independent experiments. * $P < 0.05$ and ** $P < 0.01$ using Student's *t* test

Fig. 4 Effect of Dsg2 knock-down on regulation of gene expression. **a** Western blot. A549, H1703, and H1299 cells were grown and transiently transfected with Dsg2 or negative control siRNA for 2 days and then subjected to Western blot. The data are expressed as mean \pm SE of three independent experiments. **b** Quantified data of **a**

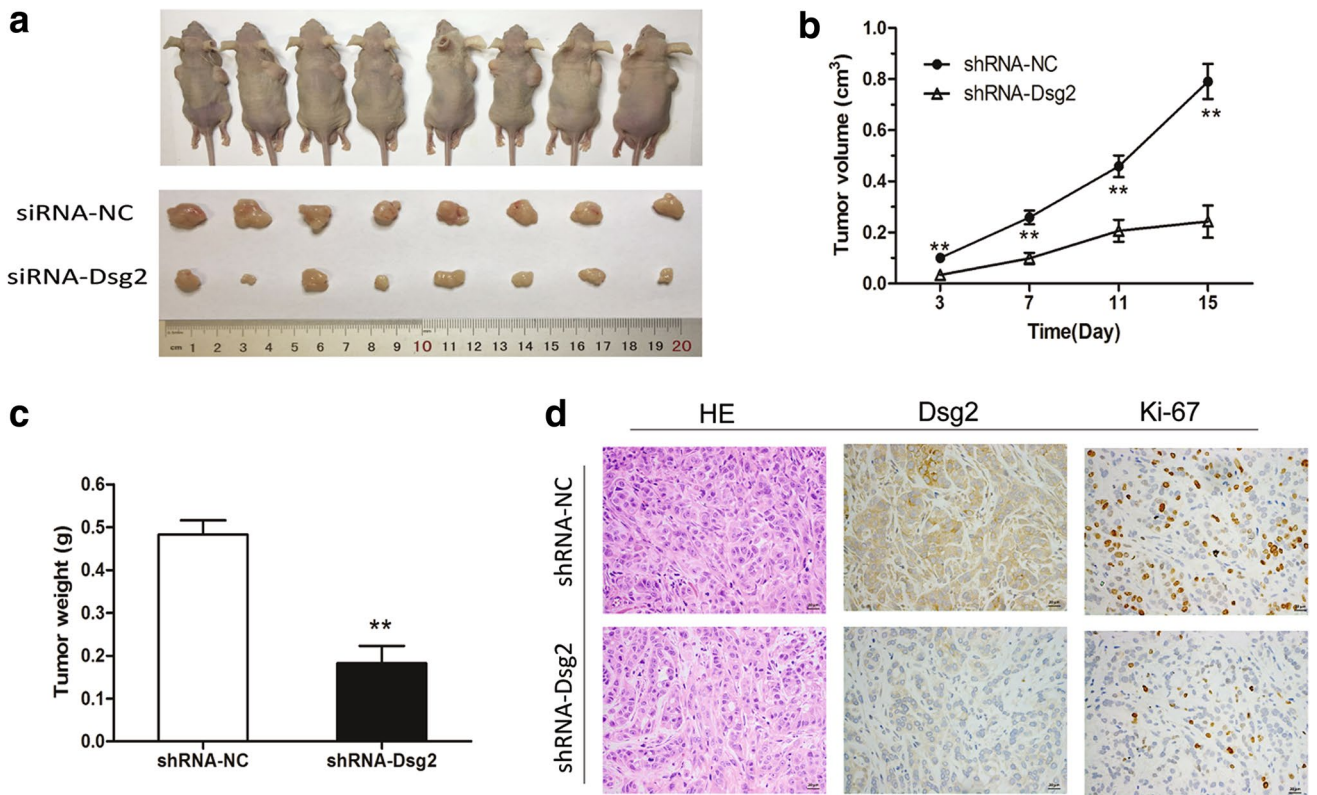
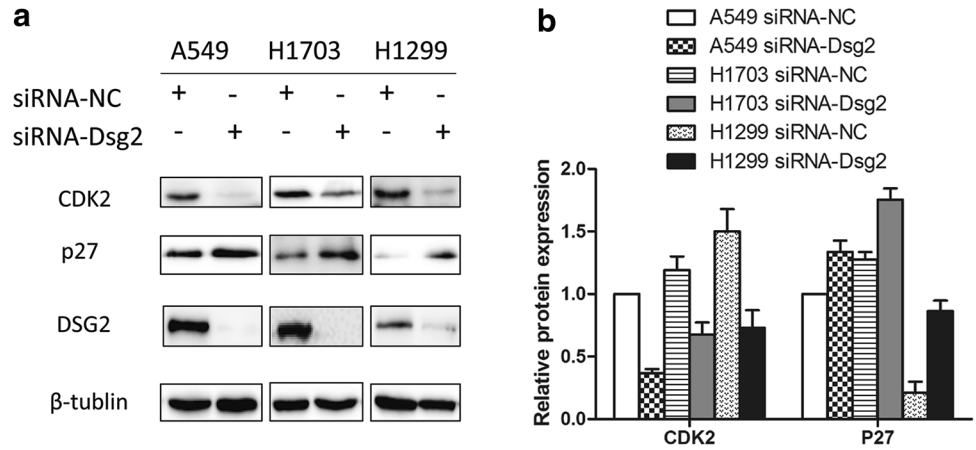


Fig. 5 Effect of Dsg2 knockdown on suppression of tumor xenograft growth in nude mice. **a** Mice and tumor xenografts. The *upper* were mice injected with A549 cells transfected with NC shRNA on the right sides of the back and Dsg2 shRNA-transfected A549 cells on the left sides of the back. **b** Tumor xenograft growth curve. **c** Tumor xenograft weight. The data are expressed as mean \pm SE of tumor vol-

umes. $**P < 0.01$ using Student's *t* test. **d** Immunohistochemistry. Tumor xenografts were subjected to tissue process and hematoxylin and eosin staining (HE) and immunohistochemistry. The representative images ($\times 400$) showed data on HE Dsg2 and Ki67 immunostaining

the paired adjacent normal lung tissues and that expression of Dsg2 was associated with a larger tumor size. Our online database analysis showed that Dsg2 expression was associated with poor prognosis in NSCLC patients, suggesting that overexpression of Dsg2 may promote NSCLC development and progression. Indeed, our current data are

consistent with another recent study showing higher Dsg2 expression in primary lung SCC (Saaber et al. 2015) and in primary and metastatic melanoma tissues (Tan et al. 2016). Dsg2 expression was associated with poor clinical outcome (Tan et al. 2016). A recent study showed that DSG2 was expressed in distinct progenitor cell subpopulations, which

was independent from its classical function as a component of desmosomes, but played a critical role in the vasculature (Ebert et al. 2016). This finding suggests that the role of Dsg2 in tumor angiogenesis could lead to tumor progression (Ebert et al. 2016; Tan et al. 2016) and may help us to understand the functions of Dsg2 in lung cancer development and progression. Moreover, in the current study, we found that Dsg2 expression was higher in lung SCC than in lung adenocarcinoma, although it was not statistically significant. This further supported data reported by Saaber et al. (2015), but was not in agreement with Fukuoka et al. (2007) who showed that levels of Dsg2 mRNA were higher in 21 lung adenocarcinomas than in 26 lung SCC. Thus, further study using a larger sample size is needed to confirm these data.

Furthermore, our *in vitro* studies demonstrated that knockdown of Dsg2 inhibited NSCLC cell proliferation and arrested NSCLC cells at the G1 phase of the cell cycle, which further supported our *ex vivo* data. In a previous study, knockdown of Dsg2 expression reduced proliferation of colon cancer cell lines *in vitro* (Kamekura et al. 2014), which is similar to our current data. Moreover, our current data also showed that knockdown of Dsg2 expression significantly inhibited growth of NSCLC cell xenografts in nude mice *in vivo*. After identifying a role for Dsg2 in NSCLC cell proliferation, we further explored the underlying molecular events and found that knockdown of Dsg2 expression downregulated CDK2 expression and upregulated p27 expression in NSCLC cells. Activation of CDK2 is essential for the G1/S transition during the cell cycle progression. CDK2 is a member of the CDK family that binds to cyclin E to drive G1 phase cells to S phase. However, a cyclin-dependent kinase inhibitor interacts with the CDK–cyclin complex to block its kinase activity. p27 (Cip2) belongs to the Cip/Kip family and can interact with the cyclin E–CDK2 complex and inhibit activity of this complex (Morgan 1997; Nomura et al. 1997). Our current data on Dsg2 knockdown–regulated gene expression indicate that Dsg2 knockdown–suppression of NSCLC cell proliferation was through targeting of p27 and CDK2. However, in other studies, many other mechanisms underlying the role of Dsg2 in tumor growth have also been reported. For example, in skin BCC and SCC, Dsg2 promoted skin tumor development through modulation of Hn signaling (Brennan-Crispi et al. 2015). Kolegraff et al. (2014) reported that Dsg2 knockdown–inhibition of cell proliferation was via phosphorylation of the epidermal growth factor receptor (EGFR) and downstream Src and Erk proteins in colon cancer cells, whereas Overmiller et al. (2016) suggested that Dsg2 knockdown in keratinocytes (HaCaT cells) inhibited EGFR expression and interfered activation of EGFR, Src, and Stat3, but not Erk or Akt. The discrepancy between Kolegraff and Overmiller’s studies could be

because Dsg2 can modulate various downstream signaling in different types of cancer cells. In other words, different transduction signaling pathways could facilitate functions of Dsg2 in different tissues and cells. Thus, in different contexts, Dsg2 may function differently to suppress or promote tumor progression.

In conclusion, our current study is the first to show that Dsg2 overexpression is involved in NSCLC tumorigenesis and the Dsg2 knockdown represses NSCLC cell proliferation *in vitro* and slowed tumor xenograft growth *in vivo*. We also showed that Dsg2 may promote tumor progression through downregulation of p27 and upregulation of CDK2. However, further mechanisms and signaling pathways underlying the role of Dsg2 in NSCLC remain to be defined.

Acknowledgments We would like to thank Dr. Zhongdong Lee of the Department of Thoracic Surgery, Jinling Hospital (Nanjing, China), for assistance in collection of tissue specimens. This study was supported in part by a Grant from the National Natural Science Foundation of China (#81470206).

Compliance with ethical standards

Conflict of interest The authors declare that there is no conflict of interest in this work.

Ethical approval All procedures performed in this study involving human participants were in accordance with the ethical standards of the institutional and/or national research committee and with the 1964 Helsinki Declaration and its later amendments or comparable ethical standards. All applicable international, national, and/or institutional guidelines for the care and use of animals were followed.

Informed consent Informed consent was obtained from all participants before conducting this study.

References

- Angst BD, Marozzi C, Magee AI (2001) The cadherin superfamily: diversity in form and function. *J Cell Sci* 114:629–641
- Barber AG, Castillo-Martin M, Bonal DM, Rybicki BA, Christiano AM, Cordon-Cardo C (2014) Characterization of desmoglein expression in the normal prostatic gland. Desmoglein 2 is an independent prognostic factor for aggressive prostate cancer. *PLoS ONE* 9:e98786. doi:10.1371/journal.pone.0098786
- Brennan D, Mahoney MG (2009) Increased expression of Dsg2 in malignant skin carcinomas: a tissue-microarray based study. *Cell Adhes Migr* 3:148–154
- Brennan-Crispi DM, Hossain C, Sahu J, Brady M, Riobo NA, Mahoney MG (2015) Crosstalk between Desmoglein 2 and Patched 1 accelerates chemical-induced skin tumorigenesis. *Oncotarget* 6:8593–8605
- Breuninger S, Reidenbach S, Sauer CG, Strobel P, Pfitzenmaier J, Trojan L, Hofmann I (2010) Desmosomal plakophilins in the prostate and prostatic adenocarcinomas: implications for diagnosis and tumor progression. *Am J Pathol* 176:2509–2519. doi:10.2353/ajpath.2010.090737

- Broussard JA, Getsios S, Green KJ (2015) Desmosome regulation and signaling in disease. *Cell Tissue Res*. doi:[10.1007/s00441-015-2136-5](https://doi.org/10.1007/s00441-015-2136-5)
- Brown L, Wan H (2015) Desmoglein 3: a help or a hindrance in cancer progression? *Cancers* 7:266–286. doi:[10.3390/cancers7010266](https://doi.org/10.3390/cancers7010266)
- Chen W et al (2016) Cancer statistics in China, 2015. *CA Cancer J Clin* 66:115–132. doi:[10.3322/caac.21338](https://doi.org/10.3322/caac.21338)
- Davies E, Cochrane R, Hiscox S, Jiang W, Sweetland H, Mansel R (1997) The role of desmoglein 2 and E-cadherin in the invasion and motility of human breast cancer cells. *Int J Oncol* 11:415–419
- Dusek RL, Attardi LD (2011) Desmosomes: new perpetrators in tumour suppression. *Nat Rev Cancer* 11:317–323. doi:[10.1038/nrc3051](https://doi.org/10.1038/nrc3051)
- Ebert LM et al (2016) A non-canonical role for desmoglein-2 in endothelial cells: implications for neoangiogenesis. *Angiogenesis*. doi:[10.1007/s10456-016-9520-y](https://doi.org/10.1007/s10456-016-9520-y)
- Fang Y et al (2013) Ubiquitin C-terminal Hydrolase 37, a novel predictor for hepatocellular carcinoma recurrence, promotes cell migration and invasion via interacting and deubiquitinating PRP19. *Biochim Biophys Acta* 1833:559–572. doi:[10.1016/j.bbamcr.2012.11.020](https://doi.org/10.1016/j.bbamcr.2012.11.020)
- Fang WK et al (2014) Prognostic significance of desmoglein 2 and desmoglein 3 in esophageal squamous cell carcinoma. *Asian Pac J Cancer Prev APJCP* 15:871–876
- Fukuoka J et al (2007) Desmoglein 3 as a prognostic factor in lung cancer. *Hum Pathol* 38:276–283. doi:[10.1016/j.humpath.2006.08.006](https://doi.org/10.1016/j.humpath.2006.08.006)
- Furukawa C et al (2005) Plakophilin 3 oncogene as prognostic marker and therapeutic target for lung cancer. *Cancer Res* 65:7102–7110. doi:[10.1158/0008-5472.CAN-04-1877](https://doi.org/10.1158/0008-5472.CAN-04-1877)
- Garrod D, Chidgey M (2008) Desmosome structure, composition and function. *Biochim Biophys Acta* 1778:572–587. doi:[10.1016/j.bbamem.2007.07.014](https://doi.org/10.1016/j.bbamem.2007.07.014)
- Gornowicz-Porowska J, Bowszyc-Dmochowska M, Seraszek-Jaros A, Kaczmarek E, Dmochowski M (2011) Loss of correlation between intensities of desmoglein 2 and desmoglein 3 expression in basal cell carcinomas. *Acta Dermatovenerol Croat ADC* 19:150–155
- Huang CC et al (2010) Desmoglein 3 is overexpressed in inverted papilloma and squamous cell carcinoma of sinonasal cavity. *Laryngoscope* 120:26–29. doi:[10.1002/lary.20151](https://doi.org/10.1002/lary.20151)
- Hulpiau P, van Roy F (2009) Molecular evolution of the cadherin superfamily. *Int J Biochem Cell Biol* 41:349–369. doi:[10.1016/j.biocel.2008.09.027](https://doi.org/10.1016/j.biocel.2008.09.027)
- Iwatsuki K, Han GW, Fukuti R, Ohtsuka M, Kikuchi S, Akiba H, Kaneko F (1999) Internalization of constitutive desmogleins with the subsequent induction of desmoglein 2 in pemphigus lesions. *Br J Dermatol* 140:35–43
- Jemal A, Bray F, Center MM, Ferlay J, Ward E, Forman D (2011) Global cancer statistics. *CA Cancer J Clin* 61:69–90. doi:[10.3322/caac.20107](https://doi.org/10.3322/caac.20107)
- Jiang R, Shi Z, Johnson JJ, Liu Y, Stack MS (2011) Kallikrein-5 promotes cleavage of desmoglein-1 and loss of cell-cell cohesion in oral squamous cell carcinoma. *J Biol Chem* 286:9127–9135. doi:[10.1074/jbc.M110.191361](https://doi.org/10.1074/jbc.M110.191361)
- Johnson JL, Najor NA, Green KJ (2014) Desmosomes: regulators of cellular signaling and adhesion in epidermal health and disease. *Cold Spring Harb Perspect Med* 4:a015297. doi:[10.1101/cshperspect.a015297](https://doi.org/10.1101/cshperspect.a015297)
- Kamekura R, Kolegraff KN, Nava P, Hilgarth RS, Feng M, Parkos CA, Nusrat A (2014) Loss of the desmosomal cadherin desmoglein-2 suppresses colon cancer cell proliferation through EGFR signaling. *Oncogene* 33:4531–4536. doi:[10.1038/onc.2013.442](https://doi.org/10.1038/onc.2013.442)
- Kolegraff K, Nava P, Laur O, Parkos CA, Nusrat A (2011) Characterization of full-length and proteolytic cleavage fragments of desmoglein-2 in native human colon and colonic epithelial cell lines. *Cell Adhes Migr* 5:306–314
- Morgan DO (1997) Cyclin-dependent kinases: engines, clocks, and microprocessors. *Annu Rev Cell Dev Biol* 13:261–291. doi:[10.1146/annurev.cellbio.13.1.261](https://doi.org/10.1146/annurev.cellbio.13.1.261)
- Nomura H, Sawada Y, Fujinaga K, Ohtaki S (1997) Cloning and characterization of rat p27Kip1, a cyclin-dependent kinase inhibitor. *Gene* 191:211–218
- Overmiller AM et al (2016) c-Src/Cav1-dependent activation of the EGFR by Dsg2. *Oncotarget*. doi:[10.18632/oncotarget.7675](https://doi.org/10.18632/oncotarget.7675)
- Pilichou K et al (2006) Mutations in desmoglein-2 gene are associated with arrhythmogenic right ventricular cardiomyopathy. *Circulation* 113:1171–1179. doi:[10.1161/CIRCULATIONAHA.105.583674](https://doi.org/10.1161/CIRCULATIONAHA.105.583674)
- Ramani VC, Hennings L, Haun RS (2008) Desmoglein 2 is a substrate of kallikrein 7 in pancreatic cancer. *BMC Cancer* 8:373. doi:[10.1186/1471-2407-8-373](https://doi.org/10.1186/1471-2407-8-373)
- Saaber F, Chen Y, Cui T, Yang L, Mireskandari M, Petersen I (2015) Expression of desmogleins 1-3 and their clinical impacts on human lung cancer. *Pathol Res Pract* 211:208–213. doi:[10.1016/j.prp.2014.10.008](https://doi.org/10.1016/j.prp.2014.10.008)
- Savci-Heijink CD, Kosari F, Aubry MC, Caron BL, Sun Z, Yang P, Vasmataz G (2009) The role of desmoglein-3 in the diagnosis of squamous cell carcinoma of the lung. *Am J Pathol* 174:1629–1637. doi:[10.2353/ajpath.2009.080778](https://doi.org/10.2353/ajpath.2009.080778)
- Schlipp A et al (2014) Desmoglein-2 interaction is crucial for cardiomyocyte cohesion and function. *Cardiovasc Res* 104:245–257. doi:[10.1093/cvr/cvu206](https://doi.org/10.1093/cvr/cvu206)
- Siegel RL, Miller KD, Jemal A (2016) Cancer statistics, 2016. *CA Cancer J Clin* 66:7–30. doi:[10.3322/caac.21332](https://doi.org/10.3322/caac.21332)
- Syrris P, Ward D, Asimaki A, Evans A, Sen-Chowdhry S, Hughes SE, McKenna WJ (2007) Desmoglein-2 mutations in arrhythmogenic right ventricular cardiomyopathy: a genotype-phenotype characterization of familial disease. *Eur Heart J* 28:581–588. doi:[10.1093/eurheartj/ehl380](https://doi.org/10.1093/eurheartj/ehl380)
- Tan LY et al (2016) Desmoglein 2 promotes vasculogenic mimicry in melanoma and is associated with poor clinical outcome. *Oncotarget*. doi:[10.18632/oncotarget.10216](https://doi.org/10.18632/oncotarget.10216)
- Torre LA, Bray F, Siegel RL, Ferlay J, Lortet-Tieulent J, Jemal A (2015) Global cancer statistics, 2012. *CA Cancer J Clin* 65:87–108. doi:[10.3322/caac.21262](https://doi.org/10.3322/caac.21262)
- Vite A et al (2013) Desmosomal cadherins are decreased in explanted arrhythmogenic right ventricular dysplasia/cardiomyopathy patient hearts. *PloS ONE* 8:e75082. doi:[10.1371/journal.pone.0075082](https://doi.org/10.1371/journal.pone.0075082)
- Yashiro M, Nishioka N, Hirakawa K (2006) Decreased expression of the adhesion molecule desmoglein-2 is associated with diffuse-type gastric carcinoma. *Eur J Cancer* 42:2397–2403. doi:[10.1016/j.ejca.2006.03.024](https://doi.org/10.1016/j.ejca.2006.03.024)